Getting the whole picture: High Content Screening using 3-dimensional cellular model systems and whole animal assays.

Janos Kriston-Vizi[a] & Horst Flotow[b]
[a] Bioinformatics Image Core, MRC Laboratory for Molecular Cell Biology, University College London, Gower Street, London, UK; [b]HDC GmbH, Byk Gulden Strasse 2, Konstanz, Germany

Abstract

Phenotypic or High Content Screening (HCS) is becoming more widely used for primary screening campaigns in drug discovery. Currently the vast majority of HCS campaigns are using cell lines grown in well-established monolayer cultures (2D tissue culture). There is widespread recognition that the more biologically relevant 3D tissue culture technologies such as spheroids and organoids and even whole animal assays will eventually be run as primary HCS. Upgrading the IT infrastructure to cope with the increase in data volumes requires investments in hardware (and software) and this will be manageable. However, the main bottleneck for the effective adoption and use of 3D tissue culture and whole animal assays in HCS is anticipated to be the development of software for the analysis of 3D images. In this review we summarize the current state of the available software and how they may be applied to analyzing 3D images obtained from a HCS campaign.

Introduction

High-Throughput Screening (HTS) is a process used routinely in early stage drug discovery. Employing a range of miniaturized assay in microtitre plates (96, 384 or 1536 well formats) and extensive automation, HTS allows the rapid interrogation of large libraries of compounds to identify hit compounds that modulate the activity of a selected target enzymes or cellular pathways (1). Target-based HTS generally only measures a single parameter per well in each assay and the result in a cellular assay, for example, is a number representing the average effect of a compound on all the cells in that well. High-content screening (HCS) can take HTS to the next level of detail. HCS is based on automated microscopy (in 96 or 384 well microtitre plates) and uses a combination of robotics, full system automation, multi-dye fluorescence imaging and flexible algorithms to extract much more detailed cellular data (2,3). HCS quantifies the phenotypes of individual cells within each well and provides a powerful method for associating morphological changes with genes and for the prediction of functional relationships (4,5).

Most HCS is currently carried out using cells that are grown as monolayer cultures on a plastic substrate. This can be referred to as conventional or two-dimensional (2D) tissue culture. *In vivo*, cells interact with neighboring cells and extracellular matrix components, forming a unique and highly functional three-dimensional (3D) structure. Although still technically challenging to set up and run, 3D tissue culture models are slowly making their way into the HCS arena and are anticipated to take HCS to the next level through increasing physiological relevance while maintaining the ability to interrogate a large number of compounds or genes.

One of the major bottlenecks in implementing HCS of 3D tissue culture models is automated image analysis. The currently available high-content imaging software solutions are well suited for the analysis of 2D images and include commercial packages (usually from the instrumentation providers) such as Acapella/Columbus/Harmony by PerkinElmer, IN Cell Investigator by GE Healthcare Life Sciences or MetaXpress by Molecular Devices, as well as several open source alternatives, including the EBImage R package (6), ImageJ/Fiji (7), and CellProfiler (8). The automated image analysis of the packages mentioned is combined with well-established statistical methods and can be used to analyze the effects of RNAi-mediated knockdown (reviewed in (9)) and screens of small molecule chemical libraries. In contrast, analysis of 3D cell culture was originally developed for low resolution, low throughput applications and therefore currently lacks the throughput required for HCS. Given the pace of improvements in imaging instrumentation and IT infrastructure, however, it is only a matter of time before 3D cell culture models are used in HCS too.

This review will focus on existing challenges surrounding translating the 3D analysis paradigm to 3D models. This includes practical considerations around culturing and image acquisition, as well as the increased challenges around image analysis, such as segmentation and artefact handling in 3 dimensions. We review current 3D cell culture models in the context of HCS and drug discovery and provide a practical guideline for the analysis of 3D HCS, from 3D culturing, through 3D high-content imaging (HCI) to 3D High Content Analysis (HCA).

3D cell and tissue culture

I*n vitro* 3D cell and tissue culture model systems attempt to recapitulate the micro-environment, cell-cell interactions and physical or mechanical interactions that occur in cells and tissues *in vivo*. 3D cultures generally show a higher degree of morphological and functional differentiation and more closely mimic *in vivo* cellular characteristics than their conventional 2D monolayer tissue culture counterparts. Cell cultures with 3D geometry can mimic the biological processes of living tissues in a more physiological manner than a 2D cellular monolayer (27). Complete signaling pathways are activated and inactivated in different ways when a cell is grown as 2D monolayer compared to 3D culture. Thus, 3D culture models are bridging the gap between monolayer cell culture and *in vivo* animal models in terms of throughput and physiological relevance and may have improved predictive value for the *in vivo* response of compounds. In practice, 3D cellular microenvironment may be set up using a scaffold or scaffold-free/liquid-based (10,11) microenvironment. There are still considerable technical challenges to overcome before 3D tissue culture assays with sufficient throughput can be used for screening large compound libraries and the development of appropriate automated image analysis methods is another major bottleneck. When these challenges are overcome, however, the increased biological relevance of 3D culture primary screening assays will maximize the benefit of high-content screening in drug discovery (12-14).

Multicellular tumor spheroids

3D multicellular tumor spheroids (MCTS) models have been used in cancer research

(15,16) for more than forty years (17). Cancer cell lines' relative robustness in culturing lowers the adaptation barrier of MCTS in HCS but practical hurdles are still reported, such as difficulties in data acquisition and automated analysis (18).

The use of a number of cell lines in MCTS screens has been reported in the literature. 3D culture systems of MCTS have been used in an RNAi screen to assay metastatic melanoma cells (19) although the analysis was only performed on the pooled lysates of transfected cells without assessment of 3D cellular features. Another example of the use of MCTS is the use of HT-29 colorectal adenocarcinoma MCTS to investigate live bacteria as gene delivery vectors (20). Dormant cells resistant to cancer therapy can be investigated with MCTS 3D HCS systems (21) and tumor growth determinants characterized (11).

For example, MCTS can be cultured without scaffolds using low attachment U-bottom microtitre plates. In a recent study, 8 lung tumor cell lines grown as 2D monolayer cultures and 3D spheroids displayed distinct morphological and functional differences between the 2D and 3D growth (22). In general, progress in culturing spheroids in 96 or even 384 well microtitre plates has made this a practicable HTS assay method. However, the automated image analysis of spheroids still lags behind this, which is discussed in more detail below.

Organoid 3D HCS

Organoid culture models are another kind of 3D model system that may become suitable for HCS application. Organoids are mammalian 3D *in vitro* model systems of specific organs that are currently mostly derived from stem cells. As the name implies, organoids display characteristics of organs, albeit in a smaller footprint and in an *in vitro* culture system (analogous to *ex vivo* tissue culture). Although organoids are technically challenging, low throughput, lack vascularization and higher level (organism) organization, they are well-characterized, sophisticated and biologically relevant model systems with a range of potential applications in drug discovery (26).

As an example, the human mammary epithelial cell line MCF-10A forms an unstructured monolayer when cultured on adherent plastic surface, but can be grown in 3D as a model of breast tissue. The MCF-10A cells exhibit a completely different morphology when grown in a scaffold-based 3D culture e.g. on a matrix of reconstituted basement membrane derived from an Engelbreth-Holm-Swarm tumor (commercially available as Matrigel). Recapitulating *in vivo* features of breast epithelium, its polarized cells form multicellular spherical cell aggregates (organoids) with a hollow lumen (acinus, Figure 1a-e), therefore providing a more physiological structural and functional context to study gene activity (28). An RNAi screen to assay MCF-10A human mammary cell line identified genes important for proliferation and survival (29).

The MCF10DCIS.com cell line (30) models the early stage of human breast cancer (ductal carcinoma in situ, DCIS) where the hollow lumen is filled with cells that do not undergo apoptosis (31-34).

There are still a number of technological hurdles to overcome in order to generate HCS compatible models. For example, the commonly used Matrigel-coating has some disadvantages, such as batch-to-batch variability in its chemical composition, high cost and inconsistent coating thickness due to difficulties in precisely pipetting such a viscous gel-like material. Alternative methods such as egg white (35) and synthetic hydrogels (36,37) may be useful alternatives in 3D HCS, particularly if they provide an optically clear coating with as little light scattering as possible.

The hanging drop method has been proposed as an alternative way to overcome difficulties in culturing 3D spheroids tested on liver microtissues (38). Organotypic 3D

liver culture models were reviewed by LeCluyse et al. (39). Another possible future development may be the adaptation of the current “organ on-a-chip” techniques to miniaturize and improve their throughput (26).

Whole organism 3D HCS

In low-throughput 3D environments, innovations in selective plane illumination microscopy (SPIM) (40,41) and digital scanned laser light-sheet fluorescence microscopy (42) enable recording of several million positions of the spatiotemporal organization of live embryonic nuclei in Zebrafish embryos and fruit fly (43). Zebrafish are an established model system of vertebrate development in particular. Adult Zebrafish at 3-4 centimeters of length are too big to fit into the well of a microtitre plate. However, their embryos are small enough to be kept in 96 or 384 well plates and compounds may be administered by simply adding them to the water in the wells. Another obvious benefit for imaging and HCS is that the Zebrafish embryos are transparent. (44-48). Zebrafish HCS is still in its infancy and the automated image acquisition and analysis present formidable technical challenges, but solutions are starting to be put forward, such as automated feature detection (49) and orientation (50).

The *Caenorhabditis elegans* model has also be used for live HCS (51) along with the generation of a 3D segmentation pipeline (52), however the computationally expensive and parameter rich active contours algorithm might not be optimal in a 3D HCS environment.

3D high-content image acquisition

This first step is currently achieved by optical sectioning (acquisition of images or optical slices of a specimen), usually using a confocal microscope. There is an ever growing list of confocal high-content imaging platforms (16,53), that are suitable for 3D HCI. For example, the PerkinElmer Opera is equipped with a spinning disk confocal microscope and has been successfully used for 3D High Content Imaging (HCI) (54), (Figure 1a-e). However, 3D HCI can be very time consuming and it can take several days to acquire the multiple optical slice image stacks in a single plate. Also, it generates vast amounts of image data that can exceed 200 gigabytes per plate. Based on the required image parameters, high content platforms can also take fewer Z-stacks and image a 384 well plate in under an hour. The minimum number of image slices depends on the macro structure. In case of 3D imaging of a live *Drosophila* embryo, acquiring 70 optical slices was necessary to collect enough information for nuclei tracking in 3D embryogenesis (55). MCTS 3D HCS can require less image slices, assuming uniform spheroid size, a few equatorial slices can present enough information for hypoxic studies or for mammary acinus luminal clearance.

Care should be taken to ensure correct autofocus as misfocus is one of the main reasons why a 3D HCS experiment may fail. Most HCS instruments allow a laser-based autofocus on the bottom of the microtiter plate, from which one can put in an offset to acquire a set of optical slices of the specimen. In addition, image-based autofocus is also possible, but may be more error-prone. Another instrument limitation in acquiring enough optical slices to reconstruct a 3D structure may be the working distance of the objective itself. A phase contrast image, combined with wide-field fluorescence HCI (e.g. IncuCyte ZOOM) can provide an alternative although lower resolution, necessitate simpler readouts such as spheroid diameter and area of projection (Figure 1f).

Hardware specifications

HCS image processing is a highly computation intensive process, and 3D HCS demands even more powerful resources. The last decades have shown steadily decreasing computer hardware prices and developments such as solid-state drives integrated on PCIe cards that facilitate 3D HCA. A common strategy to increase the speed of high-content image analysis system is to minimise the use of slow hard drives and load as many images into the computer's random access memory (RAM) as the hardware allows. Large amount of RAM in 3D HCA mean hundreds of gigabytes and even terabytes. Server-class computers are commercially available with powerful and reliable configurations that can be equipped with large amounts of RAM for 3D HCA. A sample computer configuration is reported in (54), where a system equipped with 256 gigabytes of RAM was used. That high-performance system still only allowed the processing of 6% (one row) of the 3D image data from a 384 well plate at a time. Current server configurations can accommodate total memory of up to 12 terabytes, making it more suitable for 3D HCA. Where computational speed is not a rate limiting factor, current consumer grade computers can be used for delayed batch analysis and handling basic 3D HCA and hard drives can be used as virtual memory.

Software specifications

3D high-throughput image processing and data analysis workflows are still not as widespread as 2D ones, which makes the 3D high-content morphometric analysis of intact cells or subcellular structures much more challenging. In particular, the image analysis software should be easily integrated into the HCS imaging platform. Proprietary image file formats (generated by the instruments) can be particularly troublesome here, since all images from the Z-stacks should be converted into a standard format such as ImageJ's open TIF format that can be automatically batch-processed as an image stack. In practice, many 3D cellular models are screened using 2D images from only one specific Z-plane, or a projection of the Z-stack (21,56,57). The following section describes the typical steps of a 3D HCA session. The image processing methods are approached from the 2D methods through 3D extensions to realize the potential and overcome some of the obstacles in 3D HCA applications.

Noise reduction

Image datasets often require some digital cleaning or noise reduction before segmentation. Deconvolution is an effective noise reducing method and multiple 3D deconvolution algorithms are implemented under ImageJ/Fiji (Table 1 lines 1,2). However, deconvolution has only a limited use in 3D HCS as it requires the input of multiple parameters and is computationally intensive.

Alternatively, 3D HCS can instead benefit from simpler and faster open source algorithms used in 2D image processing implemented under ImageJ/Fiji such as Median and Mean Filters, Gaussian Blur implemented by Michael Schmid and the Rolling Ball algorithm (58).

3D segmentation

Image segmentation is essentially a binary classification, where each pixel (in 2D) or voxel (in 3D) is labelled as foreground or background. The object(s) of interest are made up of foreground pixels, while background pixels form everything else.

Traditionally, 2D segmentation can be done globally using algorithms such as IsoData (59) and Otsu (60), or locally using algorithms like the Bernsen (61). The global segmentation intensity histogram-based algorithms work equally well with 3D image stacks and 2D images. However, 3D versions of effective 2D local segmentations are still missing. The 3D ImageJ Suite contains several 3D segmentation algorithms and other tools under ImageJ/Fiji and is also available as an update in Fiji (Table 1 line 3). The application of the 3D ImageJ Suite image analysis software combined with an R tool for 3D nuclear architecture quantitation, Tools for Analysis of Nuclear Genome Organization (TANGO) (62) was demonstrated on a low-throughput dataset. The next step will be the further development of these analysis tools, particularly in terms of improvements in the throughput and capacity, so they can be applied to 3D HCS.

The parameter-rich, supervised machine learning-based Trainable Weka Segmentation plugin in Fiji (Table 1 line 4) can be used for segmenting 2D images as well as 3D image stacks. However, the manual, labour-intensive training dataset generation and the computationally intensive training and prediction steps make it less feasible in a HCS environment.

Fiji's 3D Object Counter (3D-OC) (63) plugin authored by Fabrice P. Cordelieres (Table 1 line 5) contains a simple manual threshold component, which provides an adequate method of segmentation in simpler 3D HCS cases, especially when coupled with the plugin's size filter feature.

Voxel connectivity: 26 neighbour connection analysis

3D segmentation results in a set of individual foreground voxels, which must be connected in order to form 3D objects (64). A voxel can be connected to its neighbours through its faces (6-connected), faces and edges (18-connected) or its faces, edges, and corners (26-connected). The 3D-OC plugin in Fiji uses 26 neighbour connection analysis in order to label 3D objects that are separated spatially. The 2 passes connectivity analysis (especially the second pass) is time consuming, therefore currently the 3D-OC plugin's use in 3D HCS is limited by its speed.

3D distance map

3D objects located closer together than the given microscope's resolution limit can lead to artifacts, that can be separated based on their shapes. The morphology-based automated separating of erroneously merged neighboring objects is a routine task in 2D image analysis using a Euclidian Distance Map (65,66). A 3D theoretical solution for 3D is reported (67), and an open source version of this 3D algorithm is implemented under Fiji (Table 1 line 6), although it is currently labeled as

unmaintained. Thomas Boudier implemented a 3D watershed algorithm in order to split artificially merged 3D objects in ImageJ (Table 1 line 7). The application in a 3D HCS workflow is limited by the need of a seed image, the provision of which is rate limiting in a 3D HCS environment. This seed image is manually generated by the user to produce an image stack where each individual 3D object is represented by a centroid point as seed.

3D feature extraction

The 3D-OC plugin is able to measure both morphology- and intensity-based 3D features. These include volume, surface, centroid XYZ coordinates, total- and mean intensity among others. For the complete feature list and description refer to the link in Table 1 line 8. The plugin was successfully applied in a stem cell 3D HCS project (54).

In the case of texture features, 3D extensions of co-occurrence matrix and Haralick features are suggested (68) for applications in low-throughput medical imaging (69) and in higher throughput developmental biology (70). 2D projections of 3D image stacks can be analysed with Julio E. Cabrera's Texture Analyser plugin in ImageJ (Table 1 line 9) as modified by Toby C. Cornish (Table 1 line 10). Some low-throughput, open-source software including Icy (71), Vaa3D (previously called as V3D (72)) and commercial software (e.g. Amira, Imaris) have modules for 3D visualization and feature extraction (73,74). With some further development to improve the throughput, some these may become suitable for high-throughput analysis (Volocity, Definiens).

Statistical analysis of 3D features

The high-content image processing workflow results in files with large multidimensional data tables, where each 3D object (MCTS, cell or organelle) is represented by one line, its numerical fingerprint. The data analysis can routinely be performed by statistical software such as R, using cellHTS2 (75) a high-throughput analyser package that is part of the Bioconductor project (76) (Table 1 line 11). The analysis of that data requires one single value per well, therefore multiple 3D objects in multiple field of views must be averaged in a well. The robust median value is often used in a simple R script for this purpose.

3D distance matrix to calculate spatial dispersion

The quantification of 3D spatial distribution of object based on the XYZ coordinates of their 3D centroid is a frequent question in 3D HCS. It can be addressed by calculating the Euclidian distance matrix using the R function *dist()* (Table 1 line 12) and calculate the average of the distances.

Summary and future perspectives

Recent improvements in instrumentation and software have enabled the routine deployment of HCS in early stage drug discovery. Although HCS is currently mainly applied to conventional 2D cellular assays, there is software and hardware currently

available that can be adapted to enable HCS to be applied to 3D cultures as well. Figure 2 shows a summary of some workflows discussed in this review that can be applied to extend HCS to 3D cultures.

There are still significant hurdles to be overcome before sophisticated 3D and animal models can be carried out with the throughput required for HCS. However, the technological advances in automated microscopy and the associated IT infrastructure have reached a level of sophistication where almost any standard microscopic assay and analysis can be miniaturized and run as a HCS and it is anticipated that this will in time also apply to 3D cultures.

Acknowledgements

JKV was supported by the UK Medical Research Council core funding to the MRC-UCL University Unit (Ref. MC_EX_G0800785) and the European Union Seventh Framework Programme (FP7/2007-2013, grant no. PIRG08-GA-2010-276811). The help of Dr. Bernadett Kolozsvari with the image acquisition on the IncuCyte ZOOM live cell imaging system is gratefully acknowledged. We are also grateful to Dr. Jamie Freeman from Horizon Discovery for critically reading the manuscript and providing insightful comments.

Conflict of interest

The authors have no conflict of interest to declare.

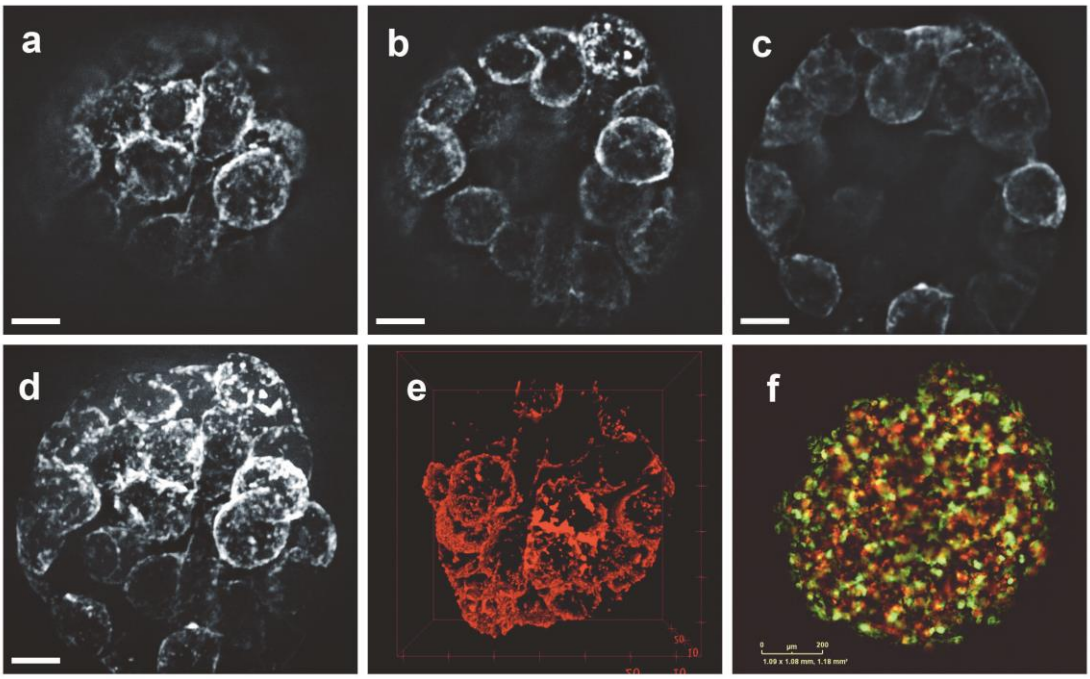

Figure 1. MCTS and organoid spheroids. (a)-(e) Acinus formed by MCF-10A mammary epithelial cells. MCF-10A cells were cultured on Matrigel for 22 days and F-actin was stained with Phalloidin. 3D image stacks were acquired with spinning disk confocal Opera LX plate reader, using a water immersion 60x (NA=1.2) lens and the following focus heights for the optical sections: (a) F = 27.5 μm, (b) F = 34.5 μm, (c) F = 44.0 μm, with hollow lumen. Panel (d) shows the maximum intensity projection of the totally acquired 57 optical slices. Scale bars: 10 μm. (e) 3D rendered visualization of the acinus shown on (a)-(e). Panel (f) shows an MCTS spheroid grown using A549 LC3-eGFP-mCherry lung cancer cells, cultured in U-bottom well and imaged with IncuCyte ZOOM system.

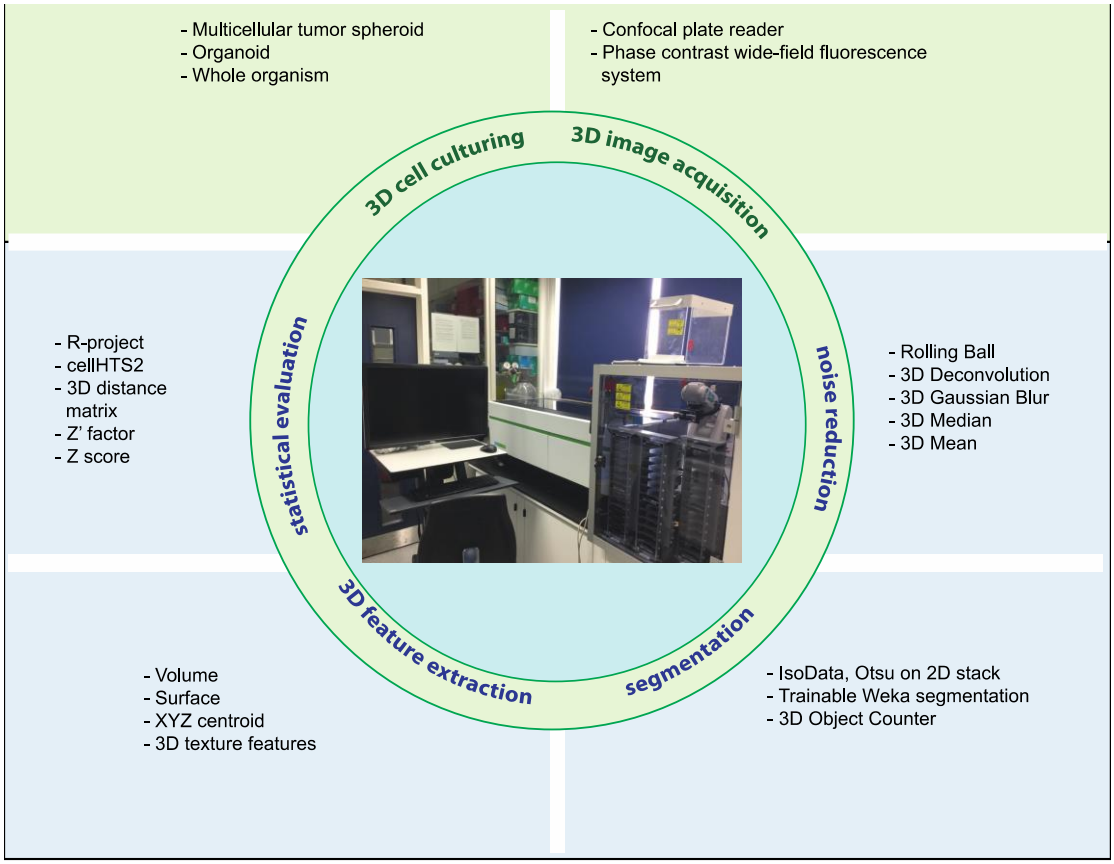

Figure 2. Diagram outlining a practical 3D HCS workflow using existing software and hardware including an Opera Phenix high-content screening system (PerkinElmer). Details are described in the accompanying text.

Table 1. Website links of 3D HCS software tools. All links were retrieved on the 9th of June 2016.

		Website URL
1	Parallel Iterative Deconvolution plugin	http://fiji.sc/Parallel_Iterative_Deconvolution
2	Iterative Deconvolve 3D	http://www.optinav.com/Iterative-Deconvolve-3D.htm
3	3D ImageJ Suite	http://imagejdocu.tudor.lu/doku.php?id=plugin:stacks:3d_ij_suite:start
4	Trainable Weka Segmentation	http://fiji.sc/Trainable_Weka_Segmentation
5	3D Object Counter	http://fiji.sc/3D_Objects_Counter
6	Distance Transform 3D	http://fiji.sc/Distance_Transform_3D
7	3D Watershed tutorial	http://imagejdocu.tudor.lu/doku.php?id=tutorial:general:watershed_3d
8	The 3D object counter plugin a.k.a 3D-OC	http://imagejdocu.tudor.lu/lib/exe/fetch.php?media=plugin:analysis:3d_object_counter:3d-oc.pdf
9	Texture Analyzer	http://rsbweb.nih.gov/ij/plugins/texture.html
10	GLCM TextureToo	http://tobycornish.com/downloads/imagej/
11	cellHTS2	https://bioconductor.org/packages/release/bioc/html/cellHTS2.html
12	dist() function	https://stat.ethz.ch/R-manual/R-devel/library/stats/html/dist.html

References

1. Entzeroth M, Flotow H, Condron P. Overview of high-throughput screening. Curr Protoc Pharmacol 2009;Chapter 9:Unit 9 4.
2. Taylor DL. Past, present, and future of high content screening and the field of cellomics. Methods Mol Biol 2007;356:3-18.
3. Giuliano KA, DeBiasio RL, Dunlay RT, Gough A, Volosky JM, Zock J, Pavlakis GN, Taylor DL. High-content screening: A new approach to easing key bottlenecks in the drug discovery process. Journal of Biomolecular Screening 1997;2:249-259.
4. Boutros M, Ahringer J. The art and design of genetic screens: RNA interference. Nat Rev Genet 2008;9:554-66.
5. Mohr S, Bakal C, Perrimon N. Genomic screening with RNAi: results and challenges. Annu Rev Biochem 2010;79:37-64.
6. Pau G, Fuchs F, Sklyar O, Boutros M, Huber W. EBImage--an R package for image processing with applications to cellular phenotypes. Bioinformatics 2010;26:979-81.
7. Abramoff MD, Magalhaes PJ, Ram SJ. Image Processing with ImageJ. Biophotonics International 2004;11:36-43.
8. Carpenter AE, Jones TR, Lamprecht MR, Clarke C, Kang IH, Friman O, Guertin DA, Chang JH, Lindquist RA, Moffat J and others. CellProfiler: image analysis software for identifying and quantifying cell phenotypes. Genome Biol 2006;7:R100.
9. Birmingham A, Selfors LM, Forster T, Wrobel D, Kennedy CJ, Shanks E, Santoyo-Lopez J, Dunican DJ, Long A, Kelleher D and others. Statistical methods for analysis of high-throughput RNA interference screens. Nat Methods 2009;6:569-75.
10. Kyburz KA, Anseth KS. Synthetic mimics of the extracellular matrix: how simple is complex enough? Ann Biomed Eng 2015;43:489-500.
11. Thoma CR, Zimmermann M, Agarkova I, Kelm JM, Krek W. 3D cell culture systems modeling tumor growth determinants in cancer target discovery. Adv Drug Deliv Rev 2014;69-70:29-41.
12. Kunz-Schughart LA, Freyer JP, Hofstaedter F, Ebner R. The use of 3-D cultures for high-throughput screening: the multicellular spheroid model. J Biomol Screen 2004;9:273-85.
13. Friedrich J, Seidel C, Ebner R, Kunz-Schughart LA. Spheroid-based drug screen: considerations and practical approach. Nat Protoc 2009;4:309-24.
14. Pampaloni F, Stelzer E. Three-dimensional cell cultures in toxicology. Biotechnol Genet Eng Rev 2010;26:117-38.
15. LaBarbera DV, Reid BG, Yoo BH. The multicellular tumor spheroid model for high-throughput cancer drug discovery. Expert Opin Drug Discov 2012;7:819-30.
16. Li L, Zhou Q, Voss TC, Quick KL, LaBarbera DV. High-throughput imaging: Focusing in on drug discovery in 3D. Methods 2015.
17. Sutherland RM, McCredie JA, Inch WR. Growth of multicell spheroids in tissue culture as a model of nodular carcinomas. J Natl Cancer Inst 1971;46:113-20.

18. Reid BG, Jerjian T, Patel P, Zhou Q, Yoo BH, Kabos P, Sartorius CA, Labarbera DV. Live multicellular tumor spheroid models for high-content imaging and screening in cancer drug discovery. Curr Chem Genom Transl Med 2014;8:27-35.
19. Gobeil S, Zhu X, Doillon CJ, Green MR. A genome-wide shRNA screen identifies GAS1 as a novel melanoma metastasis suppressor gene. Genes Dev 2008;22:2932-40.
20. Osswald A, Sun Z, Grimm V, Ampem G, Riegel K, Westendorf AM, Sommergruber W, Otte K, Durre P, Riedel CU. Three-dimensional tumor spheroids for in vitro analysis of bacteria as gene delivery vectors in tumor therapy. Microb Cell Fact 2015;14:199.
21. Wenzel C, Riefke B, Grundemann S, Krebs A, Christian S, Prinz F, Osterland M, Golfier S, Rase S, Ansari N and others. 3D high-content screening for the identification of compounds that target cells in dormant tumor spheroid regions. Exp Cell Res 2014;323:131-43.
22. Ekert JE, Johnson K, Strake B, Pardinas J, Jarantow S, Perkinson R, Colter DC. Three-dimensional lung tumor microenvironment modulates therapeutic compound responsiveness in vitro--implication for drug development. PLoS One 2014;9:e92248.
23. Tamura T, Sakai Y, Nakazawa K. Two-dimensional microarray of HepG2 spheroids using collagen/polyethylene glycol micropatterned chip. J Mater Sci Mater Med 2008;19:2071-7.
24. Kojima R, Yoshimoto K, Takahashi E, Ichino M, Miyoshi H, Nagasaki Y. Spheroid array of fetal mouse liver cells constructed on a PEG-gel micropatterned surface: upregulation of hepatic functions by co-culture with nonparenchymal liver cells. Lab Chip 2009;9:1991-3.
25. Santos E, Hernandez RM, Pedraz JL, Orive G. Novel advances in the design of three-dimensional bio-scaffolds to control cell fate: translation from 2D to 3D. Trends Biotechnol 2012;30:331-41.
26. Lancaster MA, Knoblich JA. Organogenesis in a dish: modeling development and disease using organoid technologies. Science 2014;345:1247125.
27. Pampaloni F, Reynaud EG, Stelzer EH. The third dimension bridges the gap between cell culture and live tissue. Nat Rev Mol Cell Biol 2007;8:839-45.
28. Debnath J, Muthuswamy SK, Brugge JS. Morphogenesis and oncogenesis of MCF-10A mammary epithelial acini grown in three-dimensional basement membrane cultures. Methods 2003;30:256-68.
29. Silva JM, Marran K, Parker JS, Silva J, Golding M, Schlabach MR, Elledge SJ, Hannon GJ, Chang K. Profiling essential genes in human mammary cells by multiplex RNAi screening. Science 2008;319:617-20.
30. Miller FR, Santner SJ, Tait L, Dawson PJ. MCF10DCIS.com xenograft model of human comedo ductal carcinoma in situ. J Natl Cancer Inst 2000;92:1185-6.
31. Burstein HJ, Polyak K, Wong JS, Lester SC, Kaelin CM. Ductal carcinoma in situ of the breast. N Engl J Med 2004;350:1430-41.
32. Debnath J, Brugge JS. Modelling glandular epithelial cancers in three-dimensional cultures. Nat Rev Cancer 2005;5:675-88.

33. Li Q, Mullins SR, Sloane BF, Mattingly RR. p21-Activated kinase 1 coordinates aberrant cell survival and pericellular proteolysis in a three-dimensional culture model for premalignant progression of human breast cancer. Neoplasia 2008;10:314-29.
34. Hebner C, Weaver VM, Debnath J. Modeling morphogenesis and oncogenesis in three-dimensional breast epithelial cultures. Annu Rev Pathol 2008;3:313-39.
35. Kaipparettu BA, Kuiatse I, Tak-Yee Chan B, Benny Kaipparettu M, Lee AV, Oesterreich S. Novel egg white-based 3-D cell culture system. Biotechniques 2008;45:165-8, 170-1.
36. Justice BA, Badr NA, Felder RA. 3D cell culture opens new dimensions in cell-based assays. Drug Discov Today 2009;14:102-7.
37. Caliari SR, Burdick JA. A practical guide to hydrogels for cell culture. Nat Methods 2016;13:405-14.
38. Messner S, Agarkova I, Moritz W, Kelm JM. Multi-cell type human liver microtissues for hepatotoxicity testing. Arch Toxicol 2013;87:209-13.
39. LeCluyse EL, Witek RP, Andersen ME, Powers MJ. Organotypic liver culture models: meeting current challenges in toxicity testing. Crit Rev Toxicol 2012;42:501-48.
40. Huisken J, Swoger J, Del Bene F, Wittbrodt J, Stelzer EH. Optical sectioning deep inside live embryos by selective plane illumination microscopy. Science 2004;305:1007-9.
41. Huisken J, Stainier DY. Selective plane illumination microscopy techniques in developmental biology. Development 2009;136:1963-75.
42. Keller PJ, Schmidt AD, Wittbrodt J, Stelzer EH. Reconstruction of zebrafish early embryonic development by scanned light sheet microscopy. Science 2008;322:1065-9.
43. Keller PJ, Schmidt AD, Wittbrodt J, Stelzer EH. Digital scanned laser light-sheet fluorescence microscopy (DSLM) of zebrafish and Drosophila embryonic development. Cold Spring Harb Protoc 2011;2011:1235-43.
44. Mathias JR, Saxena MT, Mumm JS. Advances in zebrafish chemical screening technologies. Future Med Chem 2012;4:1811-22.
45. Tamplin OJ, White RM, Jing L, Kaufman CK, Lacadie SA, Li P, Taylor AM, Zon LI. Small molecule screening in zebrafish: swimming in potential drug therapies. Wiley Interdiscip Rev Dev Biol 2012;1:459-68.
46. MacRae CA, Peterson RT. Zebrafish-based small molecule discovery. Chem Biol 2003;10:901-8.
47. Rubinstein AL. Zebrafish assays for drug toxicity screening. Expert Opin Drug Metab Toxicol 2006;2:231-40.
48. Rennekamp AJ, Peterson RT. 15 years of zebrafish chemical screening. Curr Opin Chem Biol 2015;24:58-70.
49. Peravali R, Gehrig J, Giselbrecht S, Lutjohann DS, Hadzhiev Y, Muller F, Liebel U. Automated feature detection and imaging for high-resolution screening of zebrafish embryos. Biotechniques 2011;50:319-24.
50. Wittbrodt JN, Liebel U, Gehrig J. Generation of orientation tools for automated zebrafish screening assays using desktop 3D printing. BMC Biotechnol 2014;14:36.
51. Muhammed M, Arvanitis M, Mylonakis E. Whole animal HTS of small molecules for antifungal compounds. Expert Opin Drug Discov 2015:1-8.

52. Chiang M, Hallman S, Cinquin A, de Mochel NR, Paz A, Kawauchi S, Calof AL, Cho KW, Fowlkes CC, Cinquin O. Analysis of in vivo single cell behavior by high throughput, human-in-the-loop segmentation of three-dimensional images. BMC Bioinformatics 2015;16:397.
53. Ketteler R, Kriston-Vizi J. High-Content Screening in Cell Biology. In: Bradshaw RA, Stahl PD, editors. Encyclopedia of Cell Biology. Volume 4. Waltham, MA: Academic Press; 2016. p 234-244.
54. Földes G, Matsa E, Kriston-Vizi J, Leja T, Amisten S, Kolker L, Kodagoda T, Dolatshad NF, Mioulane M, Vauchez K and others. Aberrant α-adrenergic hypertrophic response in Cardiomyocytes from human induced pluripotent cells. Stem Cell Reports 2014;3:905-914.
55. Kriston-Vizi J, Thong NW, Poh CL, Yee KC, Ling JSP, Kraut R, Wasser M. Gebiss: an ImageJ plugin for the specification of ground truth and the performance evaluation of 3d segmentation algorithms. Bmc Bioinformatics 2011;12.
56. Vrij EJ, Espinoza S, Heilig M, Kolew A, Schneider M, van Blitterswijk CA, Truckenmuller RK, Rivron NC. 3D high throughput screening and profiling of embryoid bodies in thermoformed microwell plates. Lab Chip 2016;16:734-42.
57. Xing J, Toh YC, Xu S, Yu H. A method for human teratogen detection by geometrically confined cell differentiation and migration. Sci Rep 2015;5:10038.
58. Sternberg SR. Biomedical Image Processing. Computer 1983;16:22-34.
59. Ridler TW, Calvard S. Picture Thresholding Using an Iterative Selection Method. Ieee Transactions on Systems Man and Cybernetics 1978;8:630-632.
60. Otsu N. Threshold Selection Method from Gray-Level Histograms. IEEE Transactions on Systems Man and Cybernetics 1979;9:62-66.
61. Bernsen J. Dynamic Thresholding of Grey-Level Images. 1986 October; Paris, France. p 1251-1255.
62. Ollion J, Cochennec J, Loll F, Escude C, Boudier T. TANGO: a generic tool for high-throughput 3D image analysis for studying nuclear organization. Bioinformatics 2013;29:1840-1.
63. Bolte S, Cordelieres FP. A guided tour into subcellular colocalization analysis in light microscopy. J Microsc 2006;224:213-32.
64. Rosenfeld A, Kak AC. Digital picture processing. New York: Academic Press; 1982.
65. Leymarie F, Levine MD. FAST RASTER SCAN DISTANCE PROPAGATION ON THE DISCRETE RECTANGULAR LATTICE. Cvgip-Image Understanding 1992;55:84-94.
66. Danielsson P-E. Euclidean distance mapping. Computer Graphics and image processing 1980;14:227-248.
67. Borgefors G. On digital distance transforms in three dimensions. Computer Vision and Image Understanding 1996;64:368-376.
68. Haralick RM, Shanmugam K, Dinstein IH. Textural Features for Image Classification. Systems, Man and Cybernetics, IEEE Transactions on 1973;SMC-3:610-621.
69. Tesar L, Smutek D, Shimizu A, Kobatake H. 3D extension of Haralick texture features for medical image analysis. Proceedings of the Fourth

IASTED International Conference on Signal Processing, Pattern Recognition, and Applications. Innsbruck, Austria: ACTA Press; 2007. p 350-355.
70. Du TH, Puah WC, Wasser M. Cell cycle phase classification in 3D in vivo microscopy of Drosophila embryogenesis. BMC Bioinformatics 2011;12 Suppl 13:S18.
71. de Chaumont F, Dallongeville S, Chenouard N, Herve N, Pop S, Provoost T, Meas-Yedid V, Pankajakshan P, Lecomte T, Le Montagner Y and others. Icy: an open bioimage informatics platform for extended reproducible research. Nat Methods 2012;9:690-6.
72. Peng H, Ruan Z, Long F, Simpson JH, Myers EW. V3D enables real-time 3D visualization and quantitative analysis of large-scale biological image data sets. Nat Biotechnol 2010;28:348-53.
73. Walter T, Shattuck DW, Baldock R, Bastin ME, Carpenter AE, Duce S, Ellenberg J, Fraser A, Hamilton N, Pieper S and others. Visualization of image data from cells to organisms. Nat Methods 2010;7:S26-41.
74. Long F, Zhou J, Peng H. Visualization and analysis of 3D microscopic images. PLoS Comput Biol 2012;8:e1002519.
75. Boutros M, Bras LP, Huber W. Analysis of cell-based RNAi screens. Genome Biol 2006;7:R66.
76. Gentleman RC, Carey VJ, Bates DM, Bolstad B, Dettling M, Dudoit S, Ellis B, Gautier L, Ge Y, Gentry J and others. Bioconductor: open software development for computational biology and bioinformatics. Genome Biol 2004;5:R80.